STRENGTH, DEFORMATION CAPACITY AND FAILURE MODE OF RC WALLS IN CYCLIC LOADING

Grammatikou, S., Biskinis, D., Fardis, M.N.
Structures Laboratory, Dept. of Civil Engineering, University of Patras, 26504, Greece

Abstract

A database of 621 cyclic tests of RC walls is utilized to evaluate past models for the cyclic strength and deformation capacity of the wall and to develop/calibrate new ones. From the observed damage the failure mode is classified as in flexure, diagonal tension or compression before or after flexural yielding, or in sliding shear. Past models being evaluated on the basis of the tests include models proposed by two of the authors and adopted in Eurocode 8-Part 3 and/or MC2010 for (a) flexural strength, (b) the cyclic shear strength after flexural yielding (as affected by the imposed ductility demand) and (c) the cyclic chord rotation capacity in flexure. Walls with height-to-length ratio less than 1.2 are considered separately, as their shear failure requires different models: past models are commented and a new one proposed and calibrated on the basis of 130 cyclic tests of squat walls. Past models for sliding shear strength are evaluated and modified on the basis of 29 cyclic tests with that failure mode: a new model is proposed for the possibility of uncontrolled sliding during a load reversal at a point in time when the flexural crack at the base is open throughout the section and only dowel action of the still elastic vertical bars is available to resist the shear force. There is good agreement of the predicted cyclic strength and/or deformation capacity per failure mode; the prediction of the most likely mode in the tests of the database is also satisfactory.

Keywords: concrete walls, cyclic loading, seismic assessment, seismic design, shear strength, ultimate deformation

1. Introduction – Experimental database

Walls are widely used in RC buildings designed for earthquake. Their design and modeling are more complex than that of columns, because shear effects and shear failures are more common. Besides, under cyclic loading they exhibit failure modes, such as in shear-compression or by sliding shear at the base, which are rare in columns. Seismic design of walls in new building or seismic assessment of existing ones in old construction requires identifying the most likely failure mode and estimating the wall cyclic strength and deformation capacity accordingly.

This paper uses a database of over 600 cyclic tests of RC walls to evaluate past models and develop/calibrate new ones for the cyclic strength and deformation capacity of the wall. The database has been assembled at the Structures Lab of the University of Patras and is currently by far the largest of its kind. It is summarized in Tables 1 and 2 (see www.dap.series.upatras.gr for the data and references). The data include 68 specimens with hollow rectangular (box) section, more representative of bridge piers than of walls, as their geometry, reinforcement layout and failure modes resemble those of walls with I-section tested uniaxially along the web. Failure in flexure is by concrete crushing or bar fracture in the flexural plastic hinge at the base (Sect. 3); diagonal tension or compression failure is due to the cyclic decay of shear resistance after flexural yielding (Sect. 4); for squat walls failing in shear and for shear sliding, see Sections 5 and 6, respectively.

Table 1
Range and mean values of the main parameters of the specimens in the database

Parameter	278 walls with rectangular section		343 of non-rectangular section (I-, U-, T-, L-, box-section)	
	min / max	mean	min / max	mean
section depth, h (m)	0.40 / 5.53	1.369	0.2 / 3.96	1.3
shear-span-to-depth ratio, L_s/h	0.39 / 5.53	1.79	0.25 / 8.3	1.7
section aspect ratio, h/b_w	2.50 / 55.3	12.82	2 / 57	17.3
f_c (MPa)	5.2 / 109.1	33.16	13.5 / 137.5	38.5
axial-load-ratio, $N/A_g f_c$	0 / 0.86	0.09	0 / 0.5	0.06
ratio of transverse web reinforcement, ρ_w, %	0 / 2.18	0.48	0 / 3.7	0.7
total longitudinal steel ratio, ρ_{tot}, %	0.07 / 4.27	1.49	0.2 / 6.2	1.65
confinement reinforcement ratio, ρ_s, %	0 / 3.65	0.68	0 / 2.5	0.5

Table 2
Number of specimens per failure mode

Group	Failure mode	rectangular walls	non-rectangular walls	total
1	Flexural	105	55	160
2	Diagonal tension - after flexural yielding	37	44	81
3	Diagonal compression, after flexural yielding	8	54	62
4	Shear failure of squat walls	47	83	130
5	Sliding shear - after flexural yielding	13	16	29
6	No failure in test, but yielding in flexure	68	91	159

2. Moment, curvature and chord rotation at flexural yielding

A prime role of the yield moment, M_y, in the present context is as a means to identify shear failures before flexural yielding from other failure modes taking place after the wall yields in flexure: if the former mode has a shear resistance denoted by V_R, it is likely to occur if $V_R < M_y/L_s$, where L_s is the shear span (moment-to-shear-ratio) at the end section of the wall. The yield moment is computed along with, and as proportional to, the yield curvature φ_y of the section, with simple expressions based on section analysis and elastic σ-ε laws (Biskinis and Fardis, 2010a); in turn φ_y is important in the present context for the calculation of the chord rotation (: deflection of the shear span relative to the yielding end, divided by L_s) at wall yielding, θ_y, as (Biskinis and Fardis, 2010a, *fib* 2012):

$$\theta_y = \varphi_y \frac{L_s + a_V z}{3} + 0.0013 + \frac{\varphi_y d_{bl} f_{yl}}{8\sqrt{f_c}} \quad (f_{yl}, f_c \text{ in the last term in MPa}) \qquad (1)$$

where:

- $a_V z$ in the first term (reflecting flexure) is the tension shift of the moment diagram, with:
  - z = internal lever arm (: distance between the tension and compression reinforcement),
  - $a_V = 1$ if diagonal cracking precedes flexural yielding of the base section (i.e., if $V_y = M_y/L_s$ exceeds the wall shear resistance without shear reinforcement, $V_{R,c}$); otherwise, a_V=0;
- d_{bl} is the diameter of the tension vertical bars and f_{yl} their yield stress,

The last term is the fixed-end-rotation due to slippage of the tension vertical bars from their anchorage zone beyond the wall end and is neglected when such slippage is physically impossible.

In the present context θ_y is used to normalize the chord rotation demand, θ, into a corresponding ductility factor, $\mu_\theta = \theta/\theta_y$, on which the cyclic shear resistance after flexural yielding depends (see Sections 4 to 6). Besides, it is used to compute the flexure-controlled cyclic ultimate chord rotation, θ_u, as the sum of θ_y and an inelastic component, given by Eqs.(2) in Section 3.

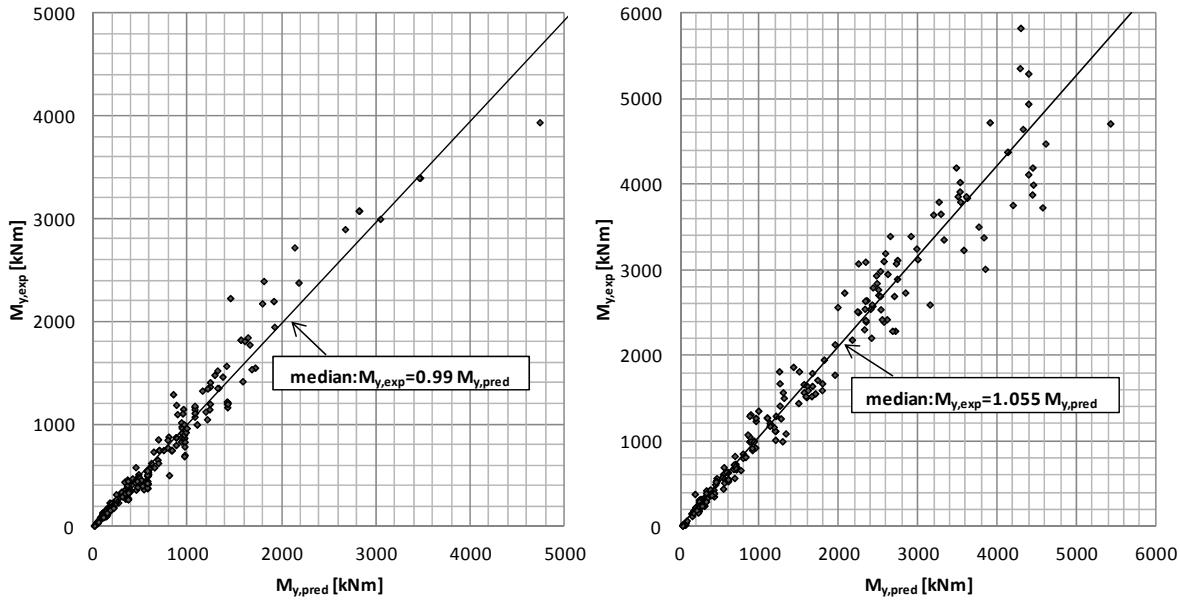

(a) (b)

Fig.1 Experimental v predicted yield moment of walls with: (a) rectangular; (b) non-rectangular section.

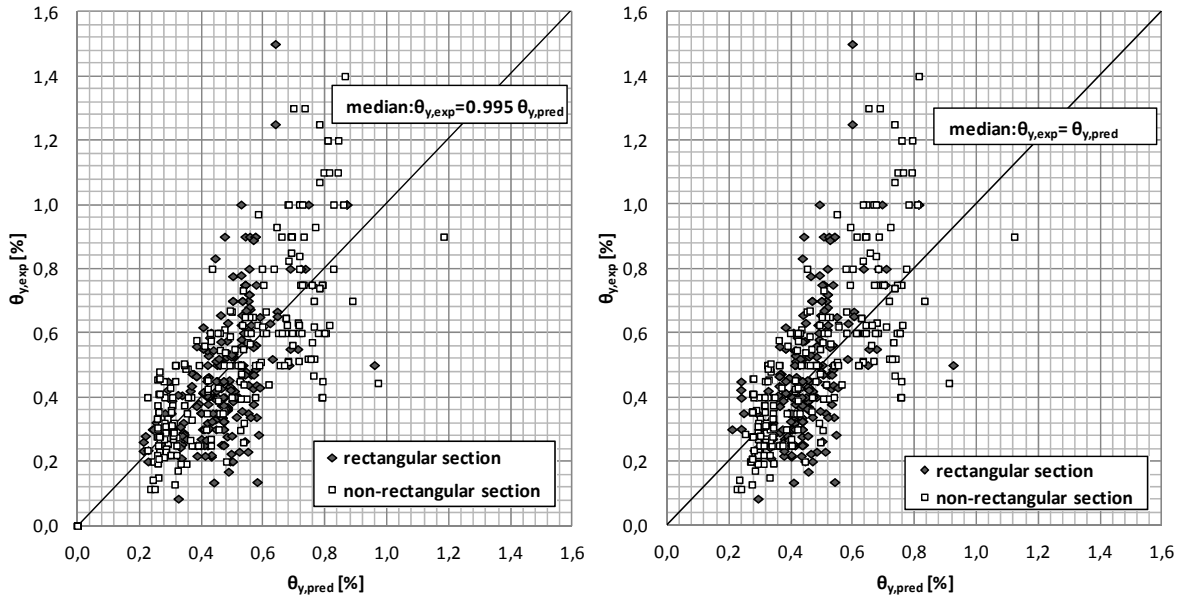

(a) (b)

Fig.2 Experimental chord rotation at yielding v prediction of: (a) Eq.(1); (b) Eq.(1) with constant term replaced by $0.0006[1+(7/6)h/L_s]$.

A bilinear approximation is commonly adopted for the monotonic moment-deflection curve of RC members up to their peak resistance, serving also as an envelope of the moment-deflection loops in cyclic loading. The corner point of the bilinear curve is identified with apparent yielding of the wall. The corner moment of the bilinear approximation of the experimental moment-deflection envelopes in the present RC wall database is the "experimental yield moment", $M_{y,exp}$, compared in Fig. 1 to the value from the simple expressions in (Biskinis and Fardis, 2010a). The value of φ_y to be used in Eq. (1) is the value computed per (Biskinis and Fardis, 2010a) as proportional to M_y times the median bias factors of 0.99 and 1.055 depicted in Fig. 1 for rectangular and non-rectangular walls, respectively. The outcome of Eq.(1) is compared in Fig. 2 to the corner chord rotation of the bilinear approximation of the experimental moment-chord rotation envelopes

("experimental chord rotation at yielding", $\theta_{y,exp}$) in the RC wall database. Grammatikou (2013) found that the same overall accuracy but better fitting of the separate groups of rectangular and non-rectangular walls is achieved, if $0.0006[1+(7/6)h/L_s]$ – with h the depth ("length") of the wall section – replaces in Eq.(1) the constant term 0.0013 of (Biskinis and Fardis, 2010a), (*fib*, 2012).

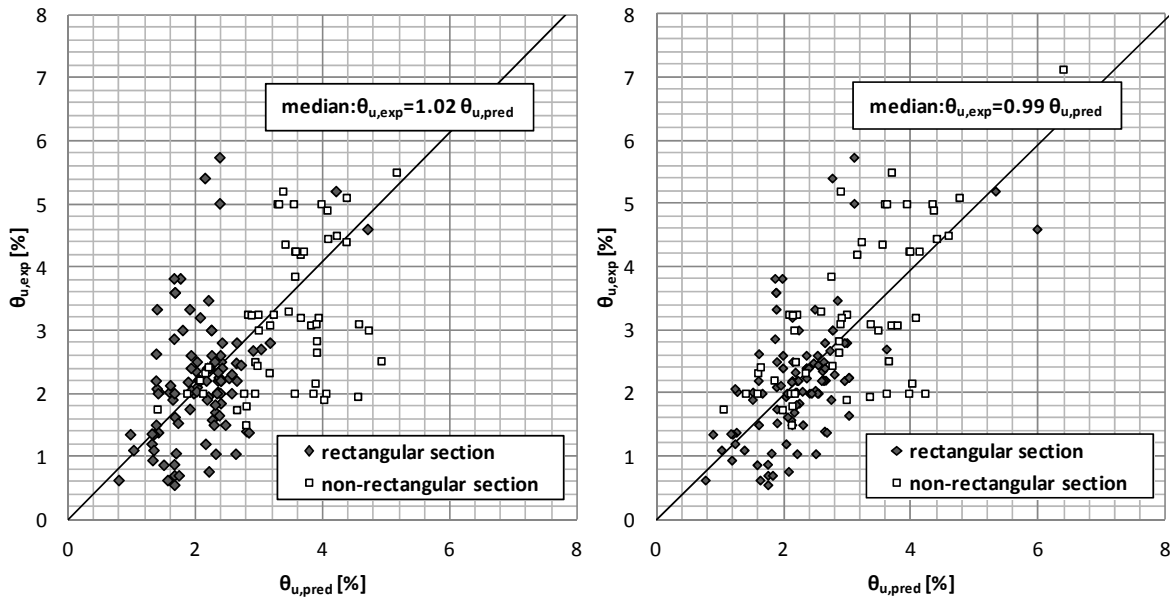

Fig.3 Experimental cyclic ultimate chord rotation v prediction of (a) Eq.(2a) (b) Eq.(2b). Group 1 in Table 2

3. Flexure-controlled ultimate chord rotation in cyclic loading

The ultimate condition and deformation (in this case chord rotation) of a RC member under cyclic loading is conventionally identified with a 20% drop in the lateral force resistance of the member compared to the peak resistance. (Biskinis and Fardis, 2010b) proposed two alternative empirical expressions – adopted in (*fib* 2012) – for the plastic part, $\theta_u^{pl} = \theta_u - \theta_y$, of the flexure-controlled cyclic ultimate chord rotation, θ_u, of rectangular RC beams, columns, walls and RC members with non-rectangular section (including a hollow rectangular one):

$$\theta_u^{pl} = \alpha_{st}^{pl}(1-0.44a_{w,r})\left(1-\frac{a_{w,nr}}{4}\right)(0.25)^{\nu}\left(\frac{\max(0.01;\omega_2)}{\max(0.01;\omega_1)}\right)^{0.3}(f_c(MPa))^{0.2}\left(\min\left(9;\frac{L_s}{h}\right)\right)^{0.35}25^{\left(\frac{\alpha\rho_w f_{yw}}{f_c}\right)}1.275^{100\rho_d} \quad (2a)$$

$$\theta_u^{pl} = \alpha_{st}^{hbw}\left(1-0.052\max\left(1.5;\min\left(10;\frac{h}{b_w}\right)\right)\right)(0.2)^{\nu}\left(\frac{\max(0.01;\omega_2)}{\max(0.01;\omega_1)}\min\left(9;\frac{L_s}{h}\right)\right)^{\frac{1}{3}}(f_c(MPa))^{0.2}25^{\left(\frac{\alpha\rho_w f_{yw}}{f_c}\right)}1.225^{100\rho_d} \quad (2b)$$

where:

for ductile (Class B, C, D) steel: $a^{pl}{}_{st} = 0.0143$, $a^{hbw}{}_{st} = 0.017$; for brittle (Class A) steel: $a^{pl}{}_{st} = 0.0069$, $a^{hbw}{}_{st} = 0.0073$;

$a_{w,r} = 1$ for rectangular walls, $a_{w,,r} = 0$ for other types of members;

$a_{w,nr} = 1$ for non-rectangular sections (T-, I-, C-, hollow rectangular); $a_{w,nr}=0$ for rectangular ones;

b_w: width of *one* web, even in cross-sections with two or more parallel webs.

$\nu = N/(bhf_c)$, with b the compression flange width and the axial force N positive for compression;

$\omega_1 = (\rho_l f_{y1}+\rho_v f_{yv})/f_c$: mechanical reinforcement ratio for the entire tension zone, including the tension flange (index 1) and the web longitudinal bars (index v);

$\omega_2 = \rho_2 f_{y2}/f_c$ mechanical reinforcement ratio for the compression flange;

ρ_d: steel ratio of diagonal bars (if any) in each diagonal direction of the member;

f_{yw}, $\rho_w = A_{sh}/b_w s_h$: yield stress of confining steel and its ratio parallel to the plane of bending;
α: confinement effectiveness factor of rectangular ties, from:

$$a = \left(1 - \frac{s_h}{2b_o}\right)\left(1 - \frac{s_h}{2h_o}\right)\left(1 - \frac{\sum b_i^2/6}{b_o h_o}\right) \quad (3)$$

with s_h denoting the centerline spacing of the ties, b_o, h_o the dimensions of the confined core to the tie centerline and b_i the on-center spacing along the section perimeter of those longitudinal bars (indexed by i) engaged by a tie corner or a cross-tie hook.

Fig. 3 compares the experimental ultimate chord rotation of the specimens in Group 1 of Table 2 – failing in flexure – to the outcome of Eqs.(2). Grammatikou (2013) found that the median bias of 2% in Fig. 3(a) is eliminated if the coefficients multiplying $a_{w,,r}$ and $a_{w,nr}$ in Eq. (2a) are reduced to 0.42 and 0.23, respectively; if $0.0006[1+(7/6)h/L_s]$ replaces the constant term 0.0013 in Eq.(1) (see end of Section 2), the 1% median bias in Fig. 3(b) disappears while the fitting of Eq. (2a) is not impaired. Witness in Fig. 3(b) the less scatter – and hence superiority – of Eq. (2b) over (2a).

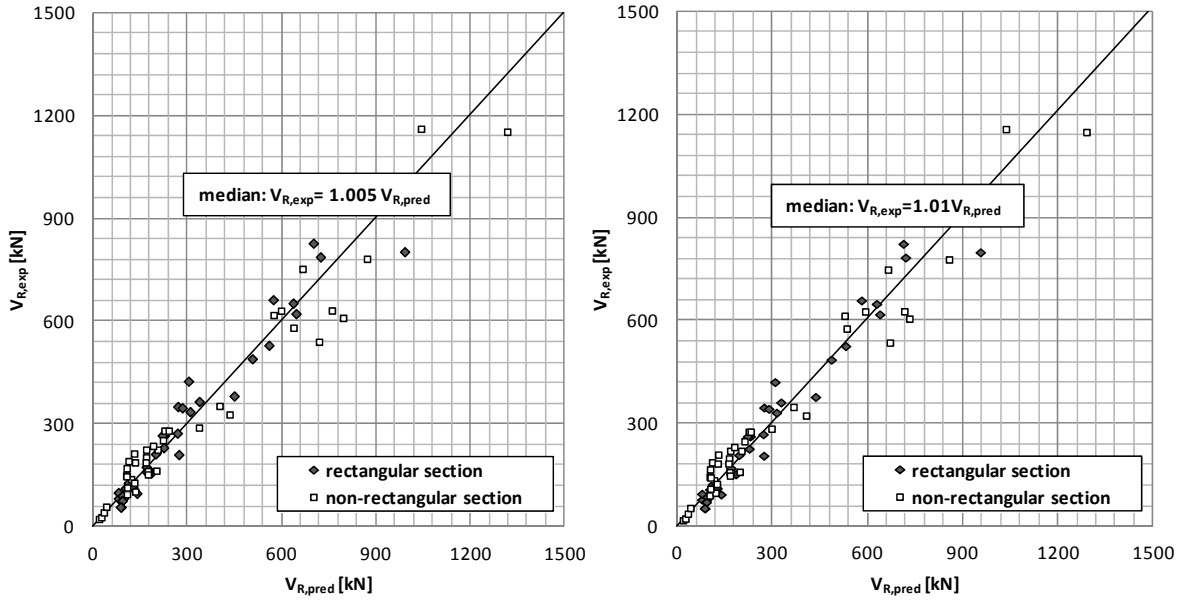

Fig.4 Experimental diagonal tension resistance after flexural yielding v prediction of (a) Eq.(4a); (b) Eq.(4b) for Group 2 of walls in Table 2

4. Cyclic shear strength of non-squat walls

4.1. Cyclic resistance in diagonal tension after flexural yielding

Once a member yields in flexure and a flexural plastic hinge forms, its shear resistance decreases with increasing inelastic cyclic displacements; so, the plastic hinge may fail in diagonal tension, before its flexure-controlled ultimate chord rotation is reached. Biskinis et al. (2004) proposed two alternative empirical models – adopted in (CEN, 2005) – for the decay of diagonal tension strength, $V_{R,ST}$, with increasing inelastic cyclic deformation (units MN, m):

$$V_{R,ST} = \frac{h-x}{2L_s}\min\left(N;0.55A_c f_c\right) + \left(1 - 0.095\min\left(5;\mu_\theta^{pl}\right)\right)\cdot 0.16\max(0.5;100\rho_{tot})\left(1 - 0.16\min\left(5;\frac{L_s}{h}\right)\right)\sqrt{f_c}\,b_w d + V_w \quad (4a)$$

$$V_{R,ST} = \frac{h-x}{2L_s}\min\left(N;0.55A_c f_c\right) + \left(1 - 0.05\min\left(5;\mu_\theta^{pl}\right)\right)\left[0.16\max(0.5;100\rho_{tot})\left(1 - 0.16\min\left(5;\frac{L_s}{h}\right)\right)\sqrt{f_c}\,b_w d + V_w\right] \quad (4b)$$

where:
$\mu_\theta^{pl}=\mu_\theta$ -1: plastic part of the ductility factor of chord rotation, with $\mu_\theta = \theta/\theta_y$ and θ_y from Eq.(1),
x: neutral axis depth at yielding per (Biskinis and Fardis, 2010a) – computed alongside M_y, φ_y, see Section 2,
A_c: area of the section,
ρ_{tot}: total longitudinal reinforcement ratio,
d: effective depth of the section,
$V_w = \rho_w b_w z f_{yw}$: contribution to shear strength of shear links having steel ρ_w and yield stress f_{yw}

As this failure mode refers to a flexural plastic hinge at the base of the wall, it can take place only after flexural yielding of the base section. So, the peak shear force in a subsequent cycle cannot exceed – at least appreciably – the shear accompanying the yield moment at the base: $V_y = M_y/L_s$. The plastic hinge may fail by diagonal tension, once the chord rotation demand, θ, increases to the point that the corresponding plastic ductility factor, $\mu_\theta^{pl} = \theta/\theta_y$ -1, causes the value of shear resistance from Eqs.(4) to drop below that of V_y.

Although fitted to a database mainly of columns and few walls, Eqs.(4) do well for the more sizeable Group 2 of walls in Table 2 which have $4.1 \geq L_s/h > 1.0$ and fail in shear tension after flexural yielding – see Fig. 4.

4.2. Cyclic shear strength in diagonal compression

After flexural yielding RC walls experience a reduction of resistance in diagonal compression with load cycling. Biskinis et al. (2004) fitted to a database of such wall failures smaller than in Group 3 of Table 2 the following empirical model – adopted in (CEN, 2005) for $L_s/h \leq 2.5$ (units MN, m):

$$V_{R,SC} = 0.85\left(1-0.06\min\left(5;\mu_\theta^{pl}\right)\right)\left(1+1.8\min\left(0.15;\frac{N}{A_c f_c}\right)\right)\left(1+0.25\max\left(1.75;100\rho_{tot}\right)\right)\left(1-0.2\min\left(2;\frac{L_s}{h}\right)\right)\sqrt{f_c}\,b_w z \quad (5)$$

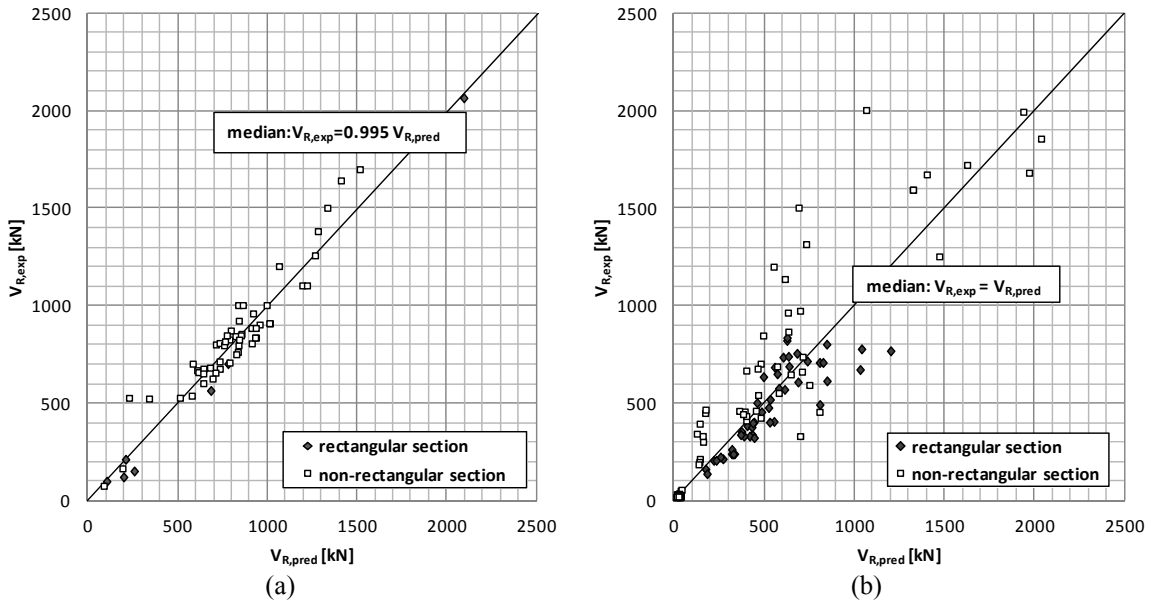

(a) (b)

Fig.5 Experimental shear resistance v predicted: (a) from Eq.(5) for walls failing in diagonal compression; (Group 3 in Table 2) (b) from Eqs.(6)-(9) for the squat walls (Group 4 in Table 2).

Fig. 5(a) shows that Eq.(5) fits well the more sizeable Group 3 in Table 2 of walls which have $2.8 \geq L_s/h > 1.0$ and which fail in diagonal compression after flexural yielding. As in the case of Eqs.(4), Eq.(5) signals shear failure when the chord rotation demand, θ, increases to the point that the corresponding plastic ductility factor, $\mu_\theta^{pl} = \theta/\theta_y$ -1, causes the value of shear resistance from Eq.(5) to drop below that of V_y.

5. Cyclic shear resistance of squat walls

For values of L_s/h of about 1.0 or less, the models in Sect. 4 exhibit a systematic and marked bias with respect to the experimental shear resistance: Eqs.(4) underestimate the post-yield cyclic strength of walls, while Eq.(5) overestimates it. So, with the few exceptions of the walls with L_s/h a little over 1.0, whose shear failure was well predicted by Eqs. (4) or (5), those that had $L_s/h \leq 1.17$ and did not fail by shear sliding (see Sect. 6 and Group 5 in Table 2) are grouped separately, as squat with shear failure (Group 4 in Table 2). A different approach is followed for them, as indeed done in (CEN, 2004) for $L_s/h < 2$ and in (ASCE, 2005) for $L_s/h < 1.5$. Note, though, that on average the (CEN, 2004) approach underestimates the cyclic shear strength of the walls in Group 4 by 90% (it is too conservative), while that of (ASCE, 2005) overestimates it by 40% (it seems unsafe).

The shear resistance fitted here to the test results of Group 4 combines (Eq. (6)):

- an empirical concrete contribution, V_c, following the format in [Barda et al., (1977)] – adopted in (ASCE, 2005) – modified here to fit the present sizeable dataset of Group 4 (see Eq.(7)), and
- a contribution, V_s, of the web reinforcement – horizontal with ratio $\rho_w = A_{sh}/b_w s_h$ and vertical with ratio $\rho_v = A_{sv}/b_w s_v$ – per Eq.(8), which extends the corresponding term in (ASCE, 2005) to account for a variable angle of the dominant crack to the vertical, θ_{cr}, per Eq.(9) (fitted to the cracking pattern at failure of the walls of Group 4).

Moreover, if the wall yields in flexure at the base before it fails in shear as squat, its shear resistance, $V_{R,squat}$, decreases with $\mu_\theta^{pl} = \mu_\theta - 1 = \theta/\theta_y - 1 \geq 0$ (with θ_y from Eq.(1)) according to Eq.(6):

$$V_{R,squat} = \left(1 - 0.07 \min\left(6; \mu_\theta^{pl}\right)\right)\left(V_c + V_s\right) \tag{6}$$

$$V_c = \left(0.52 \cdot \left(1 - 0.5\frac{L_s}{h}\right)\sqrt{f_c} + \frac{N}{4 b_w h}\right) b_w d \tag{7}$$

$$V_s = \min\left(1; \frac{L_s}{h} - 0.5\right)\rho_w b_w \min\left(L_s; \frac{h-x}{\tan\theta_{cr}}\right) f_{yw} + \min\left(1.5 - \frac{L_s}{h}; 1\right)\rho_v b_w \min\left(L_s \tan\theta_{cr}; d\right) f_{yv} \tag{8}$$

$$\theta_{cr}(^o) = 60 - 15 \min(1; L_s/h) \tag{9}$$

Eqs.(6)-(9) are meant to apply only to walls with $L_s/h < 1.2$. Unlike Eqs. (4) and (5), which apply with $\mu_\theta^{pl} = \mu_\theta - 1 = (\theta/\theta_y - 1) > 0$ after flexural yielding of the base section, Eq.(6) applies also for $\mu_\theta^{pl} = 0$, giving a cyclic shear resistance of the squat wall less than $V_y = M_y/L_s$. Fig. 5(b) compares the predictions of Eqs.(6)-(9) to the experimental shear resistance of squat walls in Group 4 of Table 2.

6. Cyclic resistance in sliding shear

Under alternating positive and negative cycles of bending that drive the wall base section past yielding, that section cracks through its full length; plastic tensile strains accumulate in the vertical bars that have yielded. Because of these strains, the crack may remain open throughout the base section, until the acting moment becomes large enough to cause the extreme bars of the compression flange to yield in compression, reversing their plastic tensile strains and closing the crack ("touch-down" moment, see below). Once the crack closes, concrete-to-concrete friction develops at the interface over the compression zone. At that stage horizontal sliding along the through-cracked base section is resisted according to Eq.(10), by the sum of:

- the friction resistance, V_f, of the compression zone, computed here with a concrete-to-concrete friction coefficient, μ_f, equal to 0.8, instead of the value of 0.6 for smooth or 0.7 for rough interfaces in (CEN 2004); the 2nd term in the (CEN 2004) expression is modified as in Eq.(11), for non-rectangular compression zones with area A_{compr} and normalised neutral axis depth ξ;
- dowel resistance, V_d, per Eq.(12), with ΣA_{sj} the area of web vertical bars ;
- the horizontal projection, V_i, of the resistance of any inclined bars, with total area (in both directions) ΣA_{si}, placed at an angle $\pm\varphi$ to the base of the wall, see Eq.(13).

$$V_{\mathrm{R,SLS}} = V_{\mathrm{f}} + V_{\mathrm{d}} + V_{\mathrm{i}} \tag{10}$$

$$V_{\mathrm{f}} = \min\left(\mu_{\mathrm{f}} \left[\left(\sum A_{\mathrm{sj}} f_{\mathrm{yl}} + N \right) \xi + \frac{M}{z} \right]; 0.3 f_{\mathrm{c}} A_{\mathrm{compr}} \right) \tag{11}$$

$$V_{\mathrm{d}} = \sum A_{\mathrm{sj}} \min\left(1.6\sqrt{f_{\mathrm{c}} f_{\mathrm{yl}}};\ f_{\mathrm{yl}} / \sqrt{3} \right) \tag{12}$$

$$V_{\mathrm{i}} = \sum A_{\mathrm{si}} f_{\mathrm{yl}} \cos\varphi \tag{13}$$

The normalised neutral axis depth, ξ, decreases as the base section proceeds from yielding to the ultimate flexural condition. Its values at these two stages, ξ_{y}, ξ_{u}, are found by section analysis with elastic σ-ε laws till yielding (cf first para. in Sect. 2 concerning calculation of M_{y}, φ_{y} per (Biskinis and Fardis, 2010a)); at ultimate, a bilinear σ-ε law is used for steel and a parabolic-rectangular one for concrete (Biskinis and Fardis, 2010b). The chord rotation at these two stages, θ_{y}, θ_{u}, may be estimated from Eqs. (1) and (2), respectively. Linear interpolation between ξ_{y}, ξ_{u} on one hand and θ_{y}, θ_{u} on the other, for the value of $\theta=(\mu_{\theta}^{\mathrm{pl}}+1)\theta_{\mathrm{y}}$ corresponding to the value of the plastic part of the chord rotation ductility factor, $\mu_{\theta}^{\mathrm{pl}}=\mu_{\theta}-1=\theta/\theta_{\mathrm{y}}-1\geq 0$, with θ_{y} from Eq.(1), gives the value of ξ to be used in Eq.(11) alongside the corresponding area A_{compr}. So, ξ decreases with increasing μ_{θ}

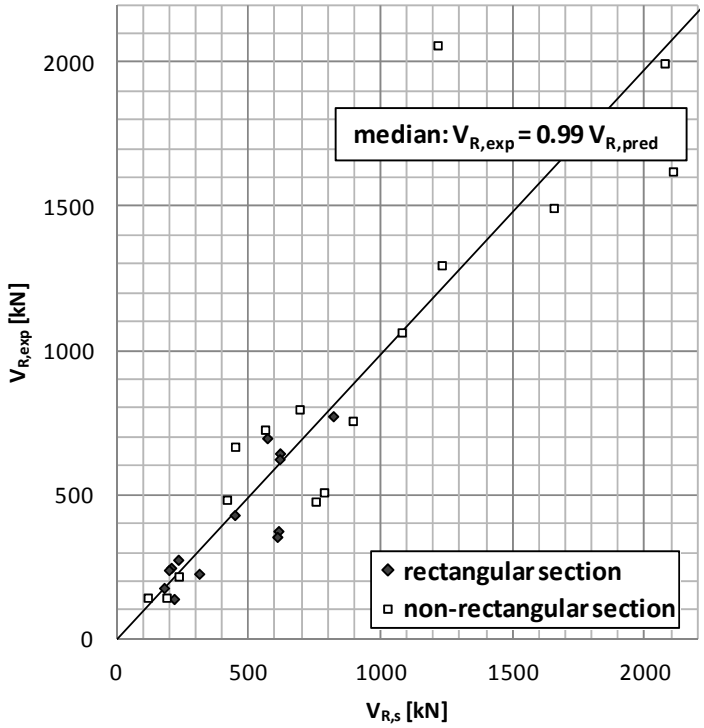

Fig.6 Experimental shear resistance of walls failing in sliding shear (Group 5 in Table 2) v prediction of Eqs.(10)-(13).

This failure mode, like those in Sect. 4, is possible only after flexural yielding at the base; before yielding the crack is not fully open through the length of the section and shear sliding cannot occur. So, like Eqs. (4) or (5), Eqs.(10) signal shear failure when the chord rotation demand, θ, increases to the point that the value of $\mu_{\theta}^{\mathrm{pl}}=\theta/\theta_{\mathrm{y}}-1$ causes that of $V_{\mathrm{R,SLS}}$ from Eqs. (10)-(13) to drop below the value of $V_{\mathrm{y}} = M_{\mathrm{y}}/L_{\mathrm{s}}$. The so-predicted $V_{\mathrm{R,SLS}}$ is compared in Fig. 6 to the experimental sliding shear resistance of the walls in Group 5 of Table 2.

Besides the possibility of full-fledged sliding at the value of $\theta=(\mu_\theta^{pl}+1)\theta_y$ that causes $V_{R,SLS}$ from Eqs. (10)-(13) to drop below $V_y = M_y/L_s$, a wall may slide prematurely, before the peak of a post-yield cycle, at a point in time when the crack is still open throughout the base section and there is no concrete-to-concrete contact yet. At that point the friction term, V_f, of Eq.(11) does not contribute to the sliding shear resistance of Eqs.(10). So, if the sum of V_d and V_i from Eqs. (12) and (13) is less than the "touch-down" shear force, $V_{td} = M_{td}/L_s$, accompanying the "touch-down" moment, M_{td}, which is necessary to close a crack open throughout the wall base section by causing the extreme bars of the compression edge to yield in compression, "premature sliding" will take place. Such sliding may be temporary, as it may be arrested when the acting shear increases to the "touch-down" value, V_{td}, activating the friction resistance, V_f.

If the axial compression is capable of causing by itself yielding of all vertical bars in the wall section, i.e., if $N > (\rho_l f_{yl}+\rho_v f_{yv}+\rho_2 f_{y2})A_c$ (in dimensionless terms, if $\nu = N/A_c f_c > \omega_l + \omega_2 + \omega_v$), then $M_{td} = 0$ and there is no possibility of "premature sliding". If $\nu < \omega_l + \omega_2 + \omega_v$, a section analysis of the through-cracked, reinforcement-only section (in fact with the reinforcement elastic) gives readily the value of M_{td} which, acting together with N, will cause the extreme bars of the compression edge to yield in compression (Grammatikou, 2013). The criterion:

$$\nu = N/A_c f_c < \omega_l + \omega_2 + \omega_v \text{ and } \quad V_{td} = M_{td}/L_s \geq V_d + V_i \tag{14}$$

may be used as supplementary to the condition: $V_y = M_y/L_s \geq V_{R,SLS}$ for shear sliding. This criterion involves only geometric and material characteristics of the wall and its axial force. Shear sliding may be considered as very likely to occur after flexural yielding at the base, if at least one of these two criteria is met.

Shear sliding is possible even in squat walls which yield in flexure before reaching the shear resistance $V_{R,squat}$ from Eqs. (6)-(9) for $\mu_\theta^{pl} = 0$. In fact, some of the walls in Group 5 have $L_s/h<1.0$.

7. Failure mode prediction

On the basis of the above, the prediction of the most likely failure mode may take place as follows:

1. The shear force at yielding, $V_y = M_y/L_s$, is found from the yield moment at the base, M_y (Sect. 2);
2. If $L_s/h \leq 1.0$, $V_{R,squat}$ is computed from Eqs. (6)-(9) for $\mu_\theta^{pl}=0$; if found less than V_y, it applies; the search ends: the wall fails in shear at a force of $V_{R,squat}(\mu_\theta^{pl}=0)$ before flexural yielding;
3. For any L_s/h, and unless the search ends in 2, Eq.(14) is checked for likely "premature sliding";
4. Unless the search has ended in 2 or 3, the ultimate chord rotation, θ_u, is calculated from Eqs.(2);
5. The θ_u-value from 4 is translated into a value of the plastic ductility factor: $\mu_\theta^{pl}=\theta_u/\theta_y - 1$;
6. Using the value of μ_θ^{pl} from 5, the following shear resistances are computed:
   a. if $L_s/h < 1.2$, $V_{R,squat}$ from Eqs. (6)-(9);
   b. if $L_s/h > 1.0$, $V_{R,ST}$ from Eqs.(4) and $V_{R,SC}$ from Eq.(5);
   c. for any L_s/h, $V_{R,SLS}$ from Eqs. (10)-(13);
7. If the lowest among the shear resistances in 6 is less than V_y, it applies, alongside the failure mode; otherwise, failure is in flexure, at a shear force of V_y and a chord rotation of θ_u;
   The outcome of this procedure for the present dataset of wall tests is shown in Table 3.

Table 3: Predicted v experimental failure mode (no. of tests)

	Experimental failure mode					**total**
Predicted failure mode	F	ST	SC	squat	SLS	**no.**
Flexure (F): Sect. 2, Eqs.(2)	149	6	6	3	2	166
Shear tension after yielding (ST): $L_s/h > 1.0$, Eqs.(4)	4	69	6	1	4	84
Shear compression after yielding (SC): $L_s/h > 1.0$, Eq.(5)	0	2	48	0	1	51
Shear, as squat: $L_s/h < 1.2$, Eqs. (6)-(9)	6	3	2	122	4	137
Sliding shear after yielding (SLS): Eqs. (10)-(13) or (12)-(14)	1	1	0	4	18	24
Total no. per experimental failure mode:	160	81	62	130	29	462

8. Conclusions

The paper has used a database of 621 cyclic tests of RC walls to evaluate past models for the wall cyclic strength and deformation capacity to develop/calibrate new ones. From the observed damage the failure mode has been classified as in flexure, diagonal tension or compression before or after flexural yielding, or in sliding shear. Expressions were developed for the corresponding limit capacities:

- in terms of cyclic deformations (chord rotations, θ) for flexure failure (θ_u, Eqs.(2) in Sect. 2);
- in terms of a shear force resistance that depends on cyclic deformations for diagonal tension ($V_{R,ST}$, Eqs.(4) in Sect. 3) or compression ($V_{R,SC}$, Eq.(5) in Sect. 4) after flexural yielding, for walls with $L_s/h > 1.0$;
- in terms of a shear force resistance that does not depend on cyclic deformations if it takes place before flexural yielding, or depends on them if it occurs after yielding ($V_{R,squat}$, Eqs. (6)-(9) in Sect. 5) for walls with $L_s/h < 1.2$ ("squat");
- in terms of a shear force resistance that depends on cyclic deformations ($V_{R,SLS}$, Eqs. (10)-(13) in Sect. 6) for shear sliding after flexural yielding, for walls with any L_s/h (with "premature sliding" as a possibility according to a criterion involving only geometric and material characteristics of the wall – Eqs. (12)-(14)).

The agreement between the predicted cyclic strength and/or deformation capacity and the observed one per failure mode is good, as demonstrated in Figs. 3-6. The prediction of the most likely mode in the tests of the database is also satisfactory, as shown in Table 3.

Acknowledgement

The research leading to these results has received funding from the European Community's 7th Framework Program [FP7/2007-2013] under grant agreement no. 227887 (SERIES) and the Hellenic General Secretariat for Research & Technology under grant ERC-12 (PRESCIENT) of the Operational Program "Education and lifelong learning", co-funded by the European Union (European Social Fund) and national resources.

References

American Society of Civil Engineers (2005) Seismic design Criteria for Structures, Systems, and Components in Nuclear Facilities (ASCE/SEI 43-05).

Barda, F., Hanson, J.M., Corley, W.G. (1977) Shear strength of low rise walls with boundary elements. *Reinforced Concrete in Seismic Zones*, SP-53, *ACI Special Publication*, 149-202.

Biskinis D., Fardis M.N. (2010a) Deformations at flexural yielding of members with continuous or lap-spliced bars. Structural Concrete; 11(3): 127-138.

Biskinis D., Fardis M.N. (2010b) Flexure-controlled ultimate deformations of members with continuous or lap-spliced bars. Structural Concrete; 11(2): 93-108.

Biskinis D., Roupakias G., Fardis M.N. (2004) Degradation of shear strength of RC members with inelastic cyclic displacements. ACI Struct J; 101(6): 773-783.

CEN (2004). European Standard EN 1998-1: Eurocode 8: Design of structures for earthquake resistance. Part 1: General rules, seismic actions and rules for buildings. Comite Europeen de Normalisation. Brussels.

CEN (2005). European Standard EN 1998-3:2005: Eurocode 8: Design of structures for earthquake resistance. Part 3: Assessment and retrofitting of buildings. Comite Europeen de Normalisation. Brussels.

fib (2012) Model Code 2010, Final draft. Bull. 65/66, Federation Internationale du Beton, Lausanne

Grammatikou S. (2013) Strength, deformation capacity and failure mode of RC walls in seismic loading. MSc Thesis, Dept. of Civil Engineering, University of Patras, Patras.